Journal of Water Process Engineering 25 (2018) 247–257

Contents lists available at ScienceDirect

Journal of Water Process Engineering

journal homepage: www.elsevier.com/locate/jwpe

Integrated use of magnetic nanostructured calcium silicate hydrate and magnetic manganese dioxide adsorbents for remediation of an acidic mine water

Alejandro Briso[a], Geraldine Quintana[a], Viviana Ide[a], Carlos Basualto[a], Lorena Molina[a], Gonzalo Montes[b], Fernando Valenzuela[a,*]

[a] Unit Operations Laboratory, Faculty of Chemical and Pharmaceutical Sciences, Universidad de Chile, Santos Dumont 964, Independencia, Santiago, Chile
[b] Minerals and Metals Characterization and Separation (M2SC) Research Group, Department of Mine Engineering, Faculty of Physical and Mathematical Sciences, Universidad de Chile, Av. Tupper 2069, Santiago, Chile

ARTICLE INFO

Keywords:
Magnetic adsorbents
Nanostructured adsorbents
Calcium silicate
Manganese dioxide
Remediation
Acid mine water

ABSTRACT

The integrated use of two solid adsorbents with magnetic properties was studied with the aim of decontaminating an acid mine water. The adsorbents were magnetic nanostructured calcium silicate hydrate (mag-NanoCSH) and magnetic manganese dioxide (mag-MnO_2), both of which consist of a crystalline Fe_3O_4 nucleus surrounded by external amorphous layers of calcium silicate and manganese oxide, respectively. They were synthesised using simple, quick, and reproducible methods. Both adsorbents were characterised chemically, physically, and magnetically via different analytical techniques. The particle size of the adsorbents varied between 60 and 200 nm, which led to a tendency to agglomerate, and the surface area varied between 30 and 70 m^2/g. The magnetic saturation of the absorbents was found to be around 57–59 emu/g, which is sufficient to ensure complete separation of these two compounds from an aqueous raffinate using a common magnet. The nanostructure and microstructure of both adsorbents had many available adsorption sites, and their chemical structure permitted efficient and simultaneous removal of cationic and anionic species present in aqueous solutions, following different adsorption mechanisms. The influence of the main variables on the adsorption of the ionic species was studied. Samples of an acid mine water were treated using both magnetic composites consecutively. In the first step, mag-NanoCSH was able to dramatically reduce the contents of many of the ions in the treated water. Then, mag-MnO_2 was added to the re-acidified raffinate produced in the first step, and the resulting final aqueous solution was found to comply with the Chilean environmental regulations.

1. Introduction

Mining and industrial operations are commonly recognised as some of the most polluting human activities. They cause numerous environmental problems, including the generation of solid and liquid wastes as well as the contamination of air by dust and gaseous emissions from pirometallurgical plants. One of the main difficulties in such cases relates to the pollution of surface and underground waters by mining and metallurgical residual effluents or their contamination with natural acid mine drainages [1]. This pollution poses both technical and economic problems. These waters contain diverse toxic contaminants, including suspended or dissolved heavy metals, anions and oxyanions as arsenates and sulphates, acidic and saline compounds, and granular and colloidal-type suspended fine solids, which are quite difficult to remove [2].

Recently, many technical options have been studied in order to remove these pollutants, mostly metallic ions and some anionic species; however, none of these treatment alternatives can be considered optimal. For example, chemical precipitation [3], ion exchange with solid resins [4], solvent extraction [5], chelation [6], biological methods [7] membranes [8] and electrochemical operations [9], among others, have been tested for removing heavy metals. Some of these alternatives are very specific and thus nearly incapable of removing different contaminants in a single process, whereas others can remove cationic species but cannot remove anionic compounds simultaneously. Moreover, some methods are expensive or impractical for use at the industrial scale.

Unquestionably, adsorption processes are some of the most

* Corresponding author.
E-mail address: fvalenzu@uchile.cl (F. Valenzuela).

https://doi.org/10.1016/j.jwpe.2018.08.010
Received 9 April 2018; Received in revised form 3 August 2018; Accepted 17 August 2018
2214-7144/ © 2018 Elsevier Ltd. All rights reserved.

promising options for removal of ionic contaminants from aqueous solutions, as many types of natural and synthetic compounds are potential absorbents. These compounds are very simple to apply, affordable, and widely available [10–15].

In this sense, a suitable industrial-scale adsorbent used to clean up polluted mining solutions must present important characteristics such as a high capacity to remove cationic and anionic species simultaneously, and easy separation from the treated water after the adsorption process. Various microparticle- and nanoparticle-type adsorbents have been prepared and modified in an attempt to improve the surface area and amount of available active adsorption sites for enhancing their efficiency in water treatment [16–18]. However, because of the tiny size of the solid formed between the adsorbent and the adsorbate species during the adsorption process, it is very difficult to separate it from the resultant raffinate aqueous solution, especially if its nature is colloidal.

A previous communication, presented the synthesis and characterisation of a nanostructured calcium silicate hydrate, unmodified or modified with Fe(III), for evaluation as an adsorbent for removing ionic species from acidic aqueous solutions [19]. The preparation of the adsorbents is simple and reproducible using low-cost commercial raw materials as lime and an industrial aqueous solution of sodium silicate. It was concluded that the presence of iron in the adsorbent structure significantly improved its ability to remove arsenic species by forming highly insoluble and stable double iron and calcium arsenate salts. However, although the solids formed in the adsorption process were very insoluble, their separation from the aqueous raffinate was troublesome. A practical solution to overcome this problem is imparting magnetic properties to the adsorbent because the magnetised structure of the adsorbent, including the composite formed with the removed species, could be easily separated from the aqueous solution by using a simple magnetic process employing a permanent magnet [20,21].

In this study, the remediation of an acid mine water samples originating from Chilean mining activity was investigated, using an integrated method with two adsorbents having magnetic properties. In the first stage, the mine water was treated with a new adsorbent prepared in our laboratory, namely a magnetic nanostructured calcium silicate hydrate (mag-NanoCSH), which can remove the highly concentrated pollutants existing in acid mine water. The preparation, characterisation, and adsorption properties of this adsorbent composite are described in Section 2.1. In the second stage, the raffinate produced during the first stage of mine water treatment with mag-NanoCSH is treated with another adsorbent, magnetic manganese dioxide (mag-MnO_2), in order for the final effluent to comply with the national Chilean environmental regulations for discharge to continental surface water bodies. A previous study reported the synthesis, characterisation, and use of this adsorbent for removing traces or low concentrations of some metallic ions from pure acid aqueous solutions [22].This adsorbent behaves as a hydrous-oxide adsorbent, which exhibits a point of zero charge (pH_{PZC}), or zeta potential, of around 3.5, allowing efficient adsorption of cationic species at pH levels above this value via an ion-exchange mechanism between the metallic ions in solution and the hydrogen ions dissociated from the surface of the adsorbent.

The adsorption mechanisms of both compounds were studied with regard to the surface area, electric charge, and chemical structure of the adsorbents. The final purpose of this practical study was to clean up the mine water effectively using both adsorbents consecutively.

2. Experimental procedure

2.1. Synthesis of the adsorbents

The synthesis of mag-NanoCSH was conducted by means of a chemical reaction between a sodium silicate solution and $Ca(OH)_2$ in the presence of HCl, as shown in equation (1). A sufficient quantity of magnetite (Fe_3O_4) was added with the purpose of imparting adsorbent magnetic properties. The synthesis is based on a procedure employed previously in the preparation of a non-modified and non-magnetic NanoCSH [23].

$$Na_2SiO_3 + Ca(OH)_2 + 2HCl \rightarrow CaSiO_{3\,(s)} + 2NaCl + 2H_2O \quad (1)$$

For the first step in the synthesis, the appropriate amount of Fe_3O_4 was added to an already prepared suspension of $Ca(OH)_2$ in water and HCl in a batch reactor under vigorous stirring at a velocity of 2000 min^{-1}. Second, sodium silicate solution was added to the reactor, and the mixture was stirred at 1500 min^{-1} for 2 h. A blackish solid corresponding to a magnetic calcium silicate hydrate was rapidly obtained and separated from the suspension using a neodymium magnet. The product was washed with water and ethanol and dried at 333 K for 12 h. In turn, the magnetic MnO_2 adsorbent was synthesised using an oxidative precipitation method in an already reported alkaline medium, in which a salt of Mn(II) was oxidised by $KMnO_4$ in the presence of magnetite (Fe_3O_4), according to the following chemical reaction [24]:

$$3MnCl_2 + 2KMnO_4 + 4OH^- \rightarrow 5MnO_2 + 2K^+ + 6Cl^- + 2H_2O \quad (2)$$

The mixture was mechanically stirred at 500 rpm for 30 min at room temperature. The use of KOH allowed it to reach pH 12, which rapidly produced a dark-brownish solid, which was separated from the solution using a neodymium magnet. The final product was washed with water and dried at 40 °C.

Both adsorbent composites, mag-NanoCSH and mag-MnO_2, have been prepared and magnetised using a commercial magnetite or Fe_3O_4 prepared at the laboratory scale [25]. Both adsorbents presented a similar adsorption capacity; thus, in this communication, all the reported results correspond to those achieved utilizing the commercial precursor.

2.2. Characterisation of the adsorbents

Different analytical techniques were used to characterize the synthesised adsorbent composites. Among them, scanning electron microscopy (SEM) and transmission electron microscopy (TEM) images were obtained using a SEM FEI Inspect F50 apparatus. The specific surface area of the particles and other porosimetry parameters were determined via Brunauer–Emmett–Teller (BET) measurements using an N_2 sorptometer at 77 K with Micrometrics ASAP 2010 equipment. The particles were also evaluated via X-ray powder diffraction (XRD) analysis, employing a Bruker D8 ADVANCE device with the purpose of verifying the crystalline or amorphous character of the solid adsorbents. The zeta potential of the mag-MnO_2 particles was determined by means of a Laser Doppler Electrophoresis method using a Malvern Mastersizer Hydro 2000MU device.

The magnetic properties of the mag-NanoCSH and mag-MnO_2 particles were determined using a vibrating sample magnetometer. The iron, manganese, and calcium contents in the adsorbents and all the metal and arsenic concentrations in the aqueous solutions in the adsorption experiments were determined by atomic absorption spectrophotometry (AAS) using a PerkinElmer PinAAcle 900 F instrument. The same technique was utilised to measure the leached metals from the adsorbent in the chemical stability tests. The Si content was measured through elemental analysis. When necessary, inductively coupled plasma mass spectrometry was used for determining lower or trace concentrations of metals in aqueous solutions.

2.3. Adsorbent stability experiments and adsorption studies

Considering that the adsorbents prepared in this study will be employed in the clean-up of acid mine water or even industrial aqueous solutions, the first experimental tests were designed to check their chemical stability towards acid aqueous solutions. The leachability of the adsorbents was evaluated as follows: 50 mg of mag-MnO_2 and

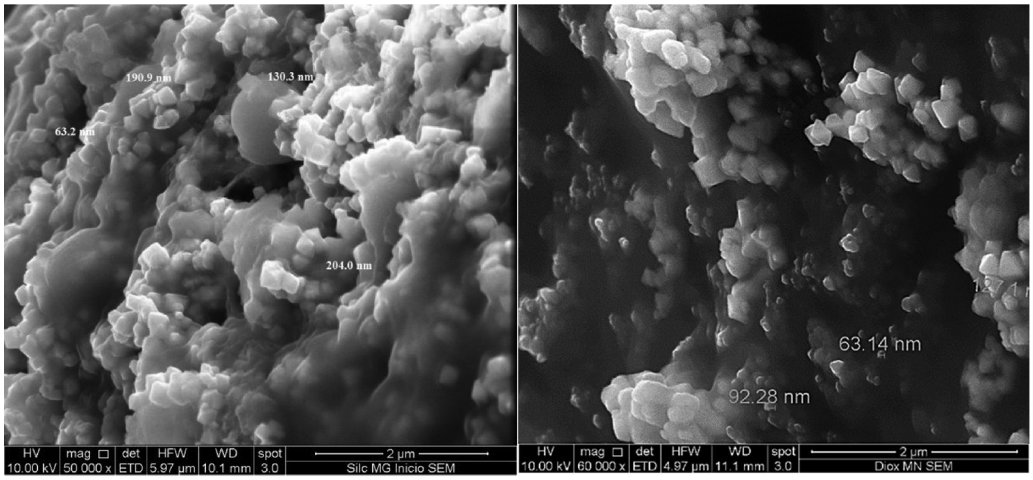

Fig. 1. SEM micrographs of the adsorbents mag-NanoCSH (a) and mag-MnO_2 (b).

100 mg of mag-NanoCSH were added to 50 mL of aqueous solutions whose initial acidities varied between pH 1 and pH 7, and mixed at 25 °C in an orbital shaker for 24 h. The pH of the acid solutions was adjusted using 0.1 M H_2SO_4 and/or 0.1 M NaOH. Once the experiments had concluded, the quantity of Ca, Mn, and Fe leached in the acid aqueous solutions was measured using AAS. The amounts of these metals remaining in the adsorbents were determined by mass balance considering their initial concentrations in the solids.

Pb(II), Cd(II), Cu(II), Zn(II), As(V), and Mo(VI) adsorption experiments were carried out at 25 °C, varying the pH and the content of the contaminants of the aqueous solutions and varying the mass of adsorbent. Some experiments were conducted using single-metal synthetic aqueous solutions prepared in the laboratory. The main experiments were carried out using samples of an acid mine water that contained, among others, all the above-mentioned chemical species. The acid mine water was a sulphated solution with a pH that varied between 2 and 4. It had the following average composition: 10.03 mg/L Pb(II), 11.87 mg/L Cd(II), 52.82 mg/L Cu(II), 43.56 mg/L Zn(II), 39.07 mg/L As(V) as arsenates, and 4.75 mg/L Mo(VI) as molybdates, and contained other components as well.

However, in some adsorption tests, the acidity of this solution and the concentrations of the ionic species were changed and adjusted to different values. Once the adsorption experiments were finalised, the pollutant-loaded solid adsorbents were easily separated from the aqueous solutions using a permanent neodymium magnet. The equilibrium pH of each resulting raffinate was measured, as were the concentrations of the ionic species that remained because they were not adsorbed. The amount of each ionic species effectively adsorbed was determined by mass balance considering their respective initial concentrations in the initial aqueous phase.

3. Results and discussion

3.1. Synthesis of the adsorbents

The synthesis of both adsorbents, mag-NanoCSH and mag-MnO_2, was very efficient, providing a high product yield. With respect to the preparation of mag-NanoCSH, for which the precursors $Ca(OH)_2$, HCl, a liquid solution of Na_2SiO_3, and commercial magnetite were used, the reaction was quick and reproducible, with an average yield of 96%, resulting in a blackish, semi-amorphous and very insoluble solid, whose particles tended to agglomerate. This solid is crystalline in nature as evidenced by its magnetite content, and it was surrounded by amorphous layers of calcium silicate. However, the sequence of adding the reagents is important. Magnetite must be added after the addition of HCl in order to avoid direct contact between both compounds, which could provoke dissolution of the iron oxide or enhance its partial oxidation to maghemite (Fe_2O_3), a species that presents a lower magnetic susceptibility than magnetite. To study the effect of the magnetic saturation degree, two different types of mag-NanoCSH adsorbents were synthesised and evaluated, with varying calcium silicate and magnetite proportions (NanoCSH/Fe_3O_4: 1/1 or 2/1). However, most of the adsorption studies were conducted using the compound NanoCSH/Fe_3O_4 at 1/1.

Similarly, the synthesis of mag-MnO_2 using the oxidative precipitation method in presence of magnetite was fast and quantitative, with a yield over 95%, resulting in a dark-brownish solid similar to MnO_2. In this case, and based on previous studies, only one type of this adsorbent was synthesised, one with a MnO_2:Fe_3O_4 proportion of 1/1, given its chemical stability and magnetic saturation.

The synthesised solids, mag-NanoCSH and mag-MnO_2, were easily separated from the reaction medium using the neodymium magnet.

3.2. Characterisation of the adsorbents

Two characterisation methodologies were used to understand the morphology of the adsorbents. Fig. 1 shows the SEM images of the unmodified nanostructured calcium silicate, mag-NanoCSH (Fig. 1a), and mag-MnO_2 (Fig. 1b). In the case of mag-NanoCSH, the morphology of particle sizes was uniform and much lower than 1 µm, illustrating their tendency to agglomerate, and some crystalline features due to the presence of Fe_3O_4 in the particles were observed. The images show individual particle sizes of around 60–200 nm for the adsorbent prepared using commercial magnetite. Fig. 1b shows an SEM micrograph of the magnetic MnO_2, wherein the particles do not have a defined geometry and correspond to very small structures whose particle size varied between 60 and 130 nm. They also presented a tendency to agglomerate. Then, the resulting compound could be classified as one having the features of a nanoadsorbent and a microadsorbent.

Fig. 2 presents the transmission electron microscopy (TEM) micrographs for both type of adsorbents, confirming the tendency of agglomeration of particles in the case of the mag-NanoCSH (Fig. 2a). The particles had a tendency to be spherical, and presented a nanostructure and a microstructure with dark central zones corresponding to a crystalline nucleus of magnetite surrounded by clearer layers of amorphous calcium silicate. The particle size of this adsorbent was confirmed in the

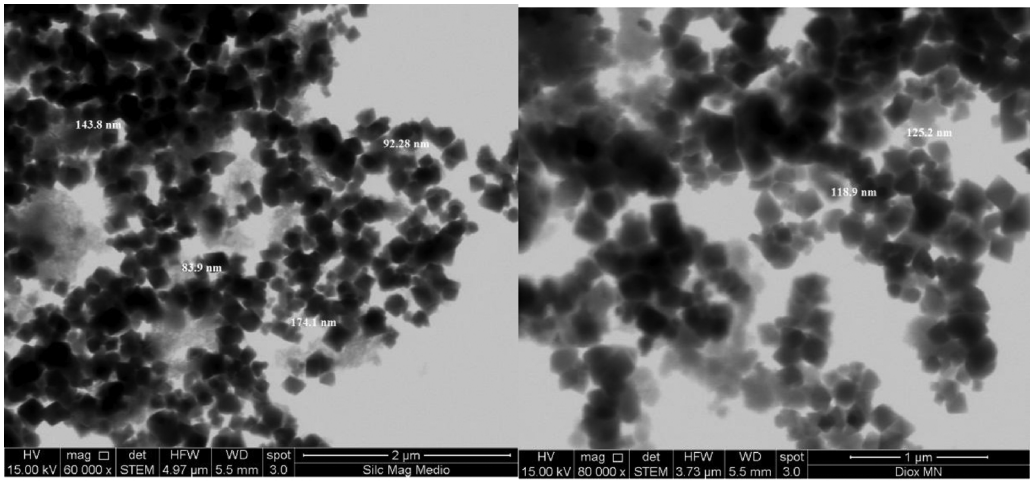

Fig. 2. TEM images of the adsorbents mag-NanoCSH (a) and mag-MnO_2 (b).

analysis, and it was dependent on the particle size of the magnetite used during the synthesis of the adsorbent. This adsorbent has a nanostructure based on a backbone of silicates, even though it might be classified as a microadsorbent in terms of particle size [23,26].

Fig. 2b shows the TEM image of the mag-MnO_2. The image shows aggregates of particles similar to those of mag-NanoCSH, that is, of a structure that poses a dark crystalline nucleus of Fe_3O_4 surrounded (in this case) by clearer amorphous layers of manganese oxide. In many cases, these particles are sized below 100 nm, with some even closer to 60 nm, which corresponds to the definition of nanoparticles. However, in a previous study, when MnO_2 was magnetised using magnetite particles prepared in the laboratory, individual particles of the adsorbent composite were even smaller than 10 nm [22]. However, the adsorption results reported hereinafter demonstrate that the low-cost adsorbents so prepared in this study were sufficiently active and adequate for removing most of the contaminants originally present in the aqueous solution.

BET porosimetry analysis measurements were carried out using an N_2 sorptometer at 77 K. The average measured surface area ranged from 30 to 40 m^2/g for mag-NanoCSH, presenting a mean pore diameter between 2 and 10 nm and an average pore volume of 0.2 cm^3/g. In the case of the magnetic manganese oxide, the surface area ranged from 60 to 70 m^2/g, with a mean pore diameter of around 5–10 nm and an average pore volume of 0.1 cm^3/g. These results ensure a vast number of available adsorption sites were distributed either in the external area or in the internal accessible area of both adsorbents types, thus ensuring efficient and fast adsorption of the ionic species existing in the aqueous solutions requiring treatment. These results also indicate that the surface area measured for mag-NanoCSH was a little smaller than that of mag-MnO_2, probably owing to the contraction of the surface generated between the bond of the nanostructured calcium silicate net with the magnetite. Moreover, the surface area and the pore diameter were affected by the size of the magnetite particles used in this study. Fig. 3 shows the adsorption-desorption isotherms for both adsorbent composites.

In both figures, the filling of the micropores and mesopores at lower relative pressure (between 0.1 and 0.8 (P/Po)), conforming to the inner structure of the adsorbent, and the filling of the macropores at higher relative pressure, corresponding to the aggregation of adsorbent particles, are observed. The macropores that originated between the particles of these aggregates were accessible to the gas but would also configure a large number of adsorption sites on the internal surface of the adsorbent, available to be filled in by the contaminants. Although both curves present a similar shape, the volume of gas adsorbed in the case of mag-NanoCSH was almost double that of mag-MnO_2, which is coherent with the bigger pore volume of the silicated compound with respect to the manganese oxide. This characteristic would probably also explain the higher adsorption capacity observed for mag-NanoCSH.

Samples of the adsorbents were subjected to X-ray powder diffraction (XRD) analysis. Fig. 4 presents the results for samples of mag-NanoCSH/Fe_3O_4 (1:1) and mag-MnO_2. The diffractogram of mag-NanoCSH (Fig. 4a) clearly shows signals at 2θ of 30°, 35°, 43°, 57°, and 63° (red), which correspond to the crystalline structure of magnetite. Moreover, the weak green signals at 2θ of 32°, 36°, and 47° are associated with $CaSiO_3$, which tends to be amorphous under the experimental route followed in this work. The low intensity of these signals confirmed the amorphous character of the external layers of $CaSiO_3$, as was seen in the SEM and TEM analyses. Besides, signals associated with calcite ($CaCO_3$) at 2θ of 29°, 39°, 47°, and 48° (blue) were observed, likely owing to impurities in the reagents used in the synthesis (lime or sodium silicate) or by carbonation from the air during the process. Thus, it is highly probable that these adsorbents would comprise a Fe_3O_4 crystalline nucleus and have external layers of amorphous calcium silicate, which is expected considering the great variety of polymeric and oligomeric species of silicates and silica existing in the Na_2SiO_3 aqueous solution, which generate colloidal solids with an untidy structure. Fig. 4b presents the XRD pattern of mag-MnO_2. This diffractogram presents newly observed, identical signals at 2θ of 30°, 35°, 43°, 57°, and 63° (red), which are attributable to the crystalline structure of Fe_3O_4. No signals corresponding to MnO_2 were observed, which is expected given the amorphous character of this compound. Hence, this adsorbent also would present a structure wherein a crystalline nucleus of magnetite is surrounded by amorphous layers of MnO_2.

The higher the magnetic saturation (Ms) of the adsorbent, the easier it was to separate it from the resulting aqueous solution (raffinate) by introducing a permanent magnet. In this sense, measurements of magnetic properties of the synthesised adsorbents are necessary. Fig. 5 shows the magnetisation curves of the prepared adsorbents and the magnetite employed in this work. In this figure, the dependence of the changes in the magnetic saturation (Ms), expressed in emu/g, was plotted against the applied magnetic field expressed in Oe (1 emu/g = 10 k Oe). It is clear that magnetite presents the highest magnetic response, at over 80 emu/g, although during the synthesis of the adsorbents, a small fraction of Fe_3O_4 was oxidised to maghemite (Fe_2O_3). As can be seen in Fig. 5, the magnetic adsorbents mag-MnO_2 and mag-

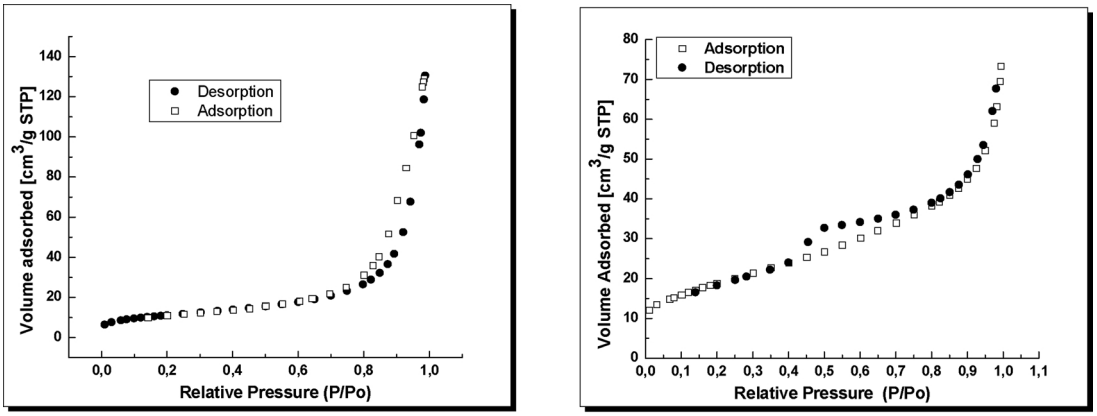

Fig. 3. Nitrogen adsorption-desorption isotherms for (a) mag-NanoCSH and (b) mag-MnO_2.

NanoCSH/Fe_3O_4 at a 1:1 ratio present a high grade of magnetic saturation, 59.35 emu/g and 57.15 emu/g respectively, which ensured complete separation of the contaminant-loaded adsorbent from the aqueous raffinate. Hence, the composite having a lower proportion of Fe_3O_4 (NanoCSH/Fe_3O_4 = 2:1) had lower magnetic saturation (42.70 emu/g), as was expected, compared to the adsorbent NanoCSH/Fe_3O_4 (=1:1), given its lower proport.

Based on TEM analysis and on the initial magnetic susceptibility obtained from Fig. 5, it is possible to make a good estimation of the layer thickness of the coatings present at the adsorbent particle composites. This was accomplished by estimating the magnetic diameter (D_m) of the particles associated to the magnetic-core of the particles using the equation derived from the Langevin function, which assumes that the magnetic nanoparticles are monodisperse [27]. As it can be seen in Fig. 5, the magnetism curves for mag-NanoCSH 1:1 and mag-MnO_2 are almost overlapped which provides a rather similar layer thickness, between 4.3 nm and 5.3 nm, for both compounds.

Undoubtedly, the calcium silicate formed during the synthesis, as well as the MnO_2, behaved as diamagnetic species, compared with behaviour of the ferromagnetic precursor Fe_3O_4. However, Fe_3O_4 by itself is not a good enough adsorbent, and thus, a suitable adsorbent composite must be structured by mixing the calcium silicate or the manganese oxide with magnetite in order to achieve an adsorbent with good adsorption capacity and sufficient magnetic properties, making feasible the separation of the loaded adsorbent from the aqueous raffinate, as was observed in this study. With regard to the particle size of the adsorbents (between 60 and 200 nm), some particles act as nanoparticles, presenting superparamagnetic properties and having almost null coercivity, which would allow their reuse in further wastewater cycles. Meanwhile, larger particles lose some of the characteristics that limit their reuse.

Complementarily, by means of the Laser Doppler Electrophoresis method, a pH_{PZC} of 3.5 was measured for MnO_2/Fe_3O_4, a value that classifies the species to be adsorbed by this compound, according to the surface charge of the adsorbent. The surface electric charge of the adsorbent is influenced by the pH of the aqueous solution. Additionally, a pH_{PZC} of 6.0 was measured for the commercial magnetite used in this study.

Chemical analysis of the main components of the adsorbent was performed. The contents of Ca, Mn, and Fe were determined by AAS of a previous acid digestion and elemental analysis of silicon content. Table 1 shows the chemical composition of the synthesised adsorbents. Adsorbent mag-NanoCSH corresponds to a calcium silicate hydrate; hence, the difference in the composition was attributed to the existence of water molecules associated with the solids. A similar condition can be assigned to mag-MnO_2, given that is a hydrous manganese oxide, which also possesses many hydroxyl groups in its structure. Table 1 shows the average composition of the different adsorbents prepared in this study in Ca, Mn, Fe, and Si.

3.3. Adsorption experiments

The adsorbents synthesised in this study were used to treat polluted acid mine waters. In this sense, they must be low-cost and also chemically and mechanically stable towards the action of acid solutions in a broad pH range, given the great variety of acid and residual mine waters. It is also possible that pollutant-loaded solid adsorbents could be desorbed using acid solutions and recycled for new adsorption processing. With this purpose, a set of experiments was designed for contacting the adsorbents with aqueous solutions whose initial pH varied between 0 and 6. Fig. 6 presents the results.

The amounts of Ca, Mn, and Fe leached were generally very low, especially over pH 2, where only a minimal concentration of these metals was dissolved. Iron is not leached at all over pH 2, probably owing to, in both adsorbents, magnetite as the nucleus of the solid surrounded by layers of calcium silicate or MnO_2, which protects it from attack by protons. Slightly higher leaching of calcium and manganese was observed, probably because they are more exposed in aqueous solutions, given the sites of the external layers of both adsorbents and owing to their solubility. Undoubtedly, when the acidity of the aqueous solution is too high, specifically at pH below 2.0, the dissolution of these metals is caused by the direct attack of the extremely high concentration of hydrogen ions on the surface of the adsorbents, promoting the leaching of the metals into and their presence in the resultant aqueous solutions. Subsequently, it can be concluded that both types of adsorbents can be used for treating polluted aqueous solutions whose acidity is not below pH 2.0. In all cases, despite the scarce dissolution of iron and other components, the solids were completely separated from the solution using a neodymium magnet; thus, the magnetic saturation of the adsorbents remained constant.

Before applying the adsorbents to the treatment of samples of actual acid mine water, a series of experiments was designed to test them using aqueous solutions that simulate mine water. The purpose was to establish the pH range in which the adsorbents presented their best adsorption capacity and to measure the contaminant-loading capacity of both compounds, defined as "*q*" and expressed in *mg ion removed/g adsorbent*. Fig. 7 shows the effect of the initial pH of the aqueous solution on the adsorption of Pb(II), Cd(II), Cu(II), and Zn(II) ions using mag-MnO_2 as the adsorbent. These experiments were carried out using aqueous solutions containing around 10 mg/L of these metallic ions,

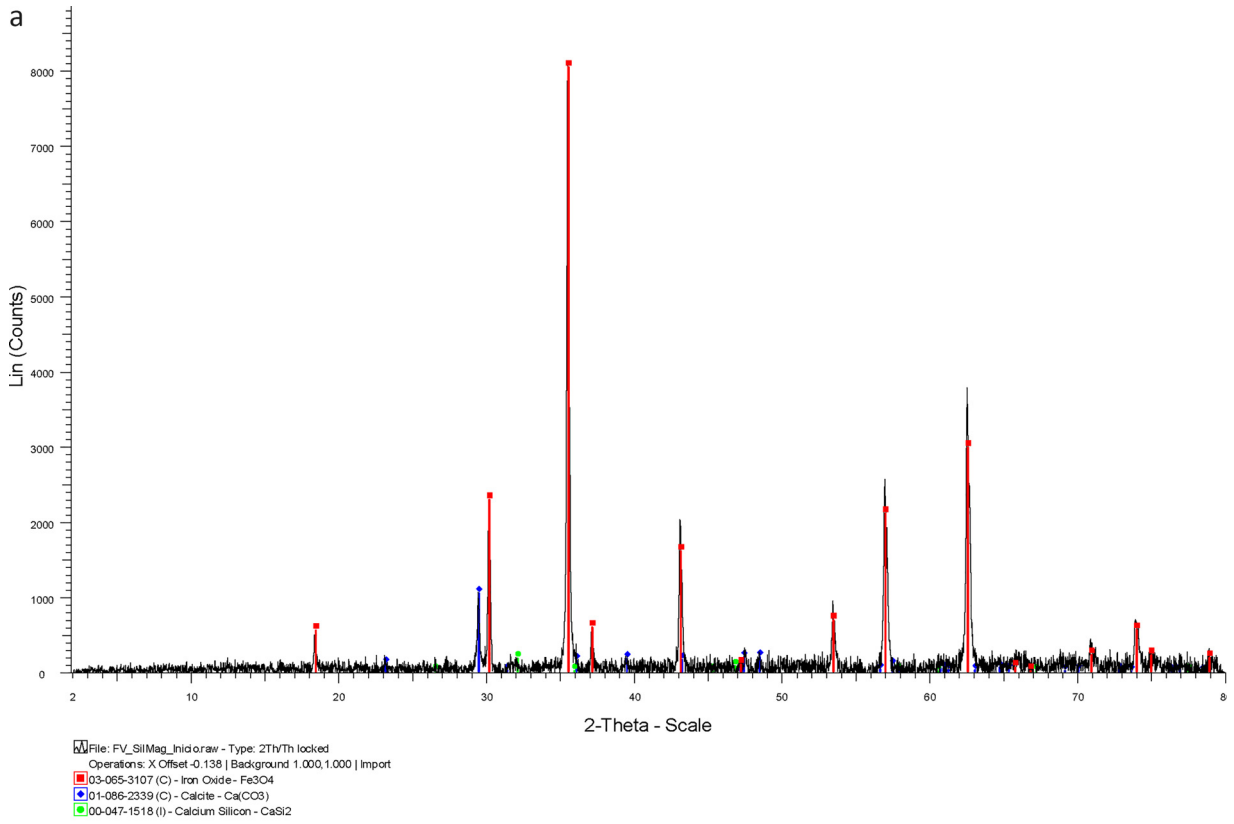

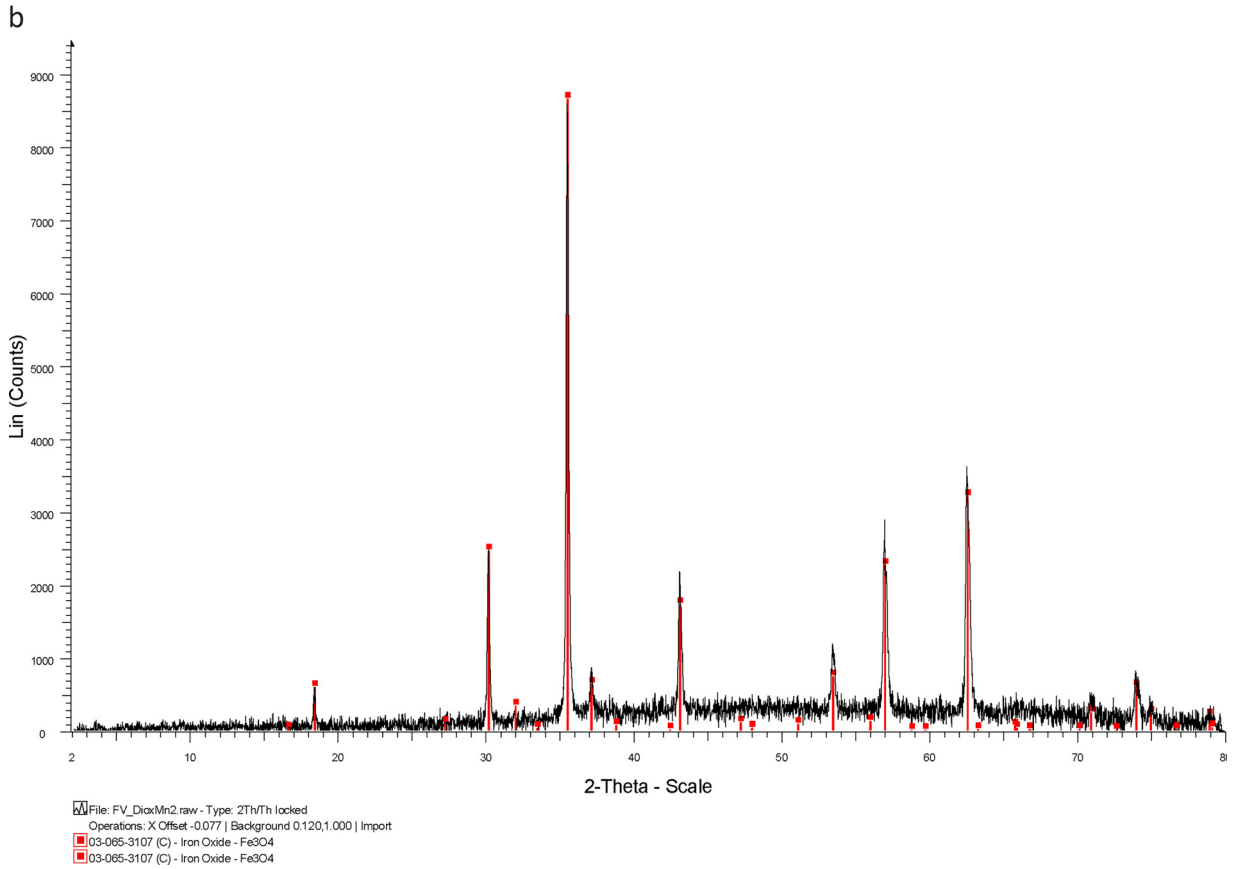

Fig. 4. (a) XRD patterns of mag-NanoCSH. (b) XRD patterns of mag-MnO_2.

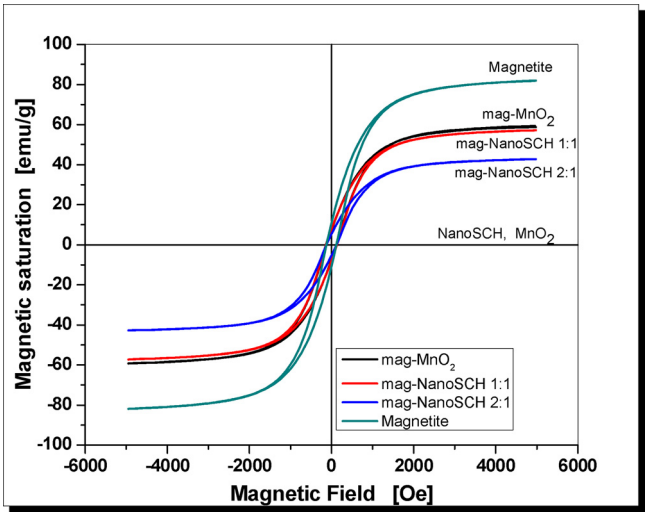

Fig. 5. Magnetisation curves of the adsorbents mag-MnO_2, mag-NanoCSH, and Fe_3O_4.

Table 1
Average composition of the synthesised adsorbents.

Adsorbent	% Ca (w/w)	% Fe (w/w)	% Si (w/w)	% Mn (w/w)
mag-MnO_2 (MnO_2/Fe_3O_4 = 1:1)	–	33.63	–	12.08
mag-NanoCSH (NanoCSH/Fe_3O_4 = 1:1)	5.96	34.03	4.13	–
mag-NanoCSH (NanoCSH/Fe_3O_4 = 2:1)	9.36	26.99	8.09	–

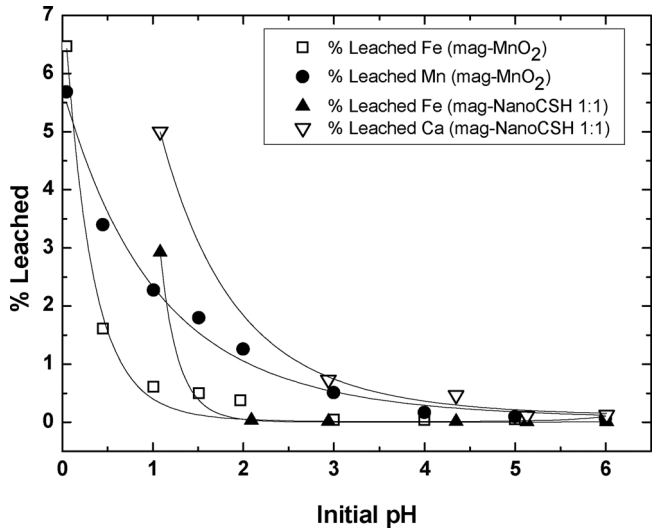

Fig. 6. Chemical stability tests of adsorbents as a function of the acidity of the aqueous solution.

which were mixed with 50 mg of mag-MnO_2.

Fig. 7 shows that as the pH of the aqueous phase increases, the extraction percentage of the four metallic species increases. This adsorbent is a magnetic hydrous oxide compound whose surface can suffer protonation or deprotonation reactions. This can be explained because the pH of zero charge (pHzc), or zeta potential, measured for this adsorbent was around 3.2–3.5. That is, the adsorption of cationic metal species increased with increasing pH of the aqueous solution, especially above the zero charge pH value (pHzc). Under this condition, the adsorption of cationic species would be favoured owing to the

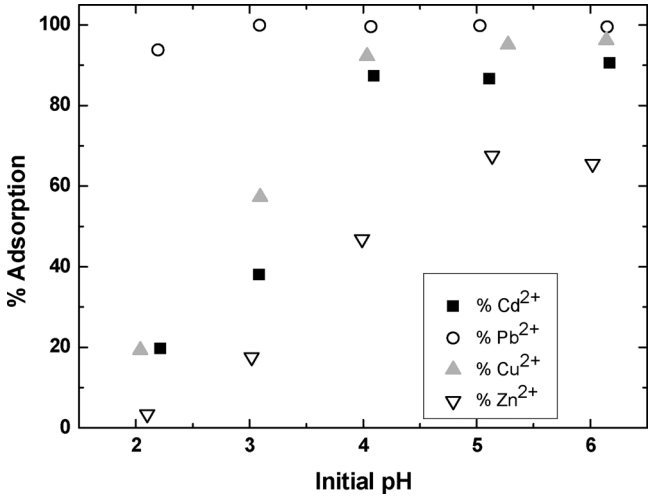

Fig. 7. Dependence of Pb(II), Cd(II), Cu(II), and Zn(II) ion adsorption onto mag-MnO_2 with initial pH.

polyhydroxylation of the surface of the adsorbent, followed by a deprotonation of the hydroxyl groups, thus favouring an adsorption mechanism governed by cation exchange between the metallic ion and the H^+ groups, as is expressed in the following equations:

$$Mn{-}OH_{(s)} + OH^-_{(aq)} \rightleftarrows [Mn{-}(OH)_{2\,(s)}]^- \quad (3)$$

$$[Mn{-}(OH)_{2\,(s)}]^- + M^{2+}_{(aq)} \rightleftarrows [Mn{-}(O^-)_2M^{2+}_{(s)}]^- + 2H^+_{(aq)} \quad (4)$$

where $Mn{-}OH_{(s)}$ represents the manganese hydrous oxide, and M is the metal ion present in the aqueous solution to be removed. With regard to the adsorption of these divalent cations, the metallic ion would coordinate with the donor oxygen atom on the surface of the adsorbent material, liberating protons to the solution [24]. On the other hand, significant adsorption at a pH lower than the zeta potential (pH < 3.2–3.5) would not have occurred, because in a sulphuric medium at least, the four metals studied would not form anionic species that would feasibly be adsorbed by MnO_2 at low pH.

Fig. 7 shows that the adsorption of Pb^{2+} is preferred over that of Cd^{2+} and Cu^{2+}, with Zn^{2+} being the least favoured. It is also observed that the adsorption of all the ions reaches a maximum around pH 4.0–5.0, and does not increase at higher pH values as the range for the deprotonation of the H^+ ions from the surface of the adsorbent is minimal. However, the acidity range of aqueous solutions between pH values of 1 and 5 is of interest in the treatment of acid mine waters. Both the acid mine drainages and the aqueous mining wastes generated in metallurgical plants are generally this acidic. Similar experiments were carried out for comparisons, but only with Fe_3O_4, observing much lower adsorption, especially at more acidic pH levels, owing not only to a lower adsorption capacity of magnetite (given its structure), but also because its pHzc is close to 6.0. The latter prevents or limits the adsorption of metal ions on its surface at pH lower than this value.

Considering that the mine water used also contained anionic species, we conducted adsorption experiments of the oxyanion arsenates and molybdates normally found in numerous acid mine waters, particularly those related to Chilean copper mining. They appear structurally associated with copper ores, chemical species such as molybdenite (MoS_2), and arsenic minerals such as enargite and tennantite. The adsorption experiments were performed by mixing 50 mg of adsorbent with a feed solution containing 10 mg/L of Mo(VI) and As(V). The results are presented in Fig. 8.

Fig. 8 shows that the adsorption of both oxyanionic species is favoured in the pH range between 1 and 2, that is, under strongly acidic conditions. This finding coincides with a pH range lower than the value measured for pHzc for this adsorbent. Under these conditions, the

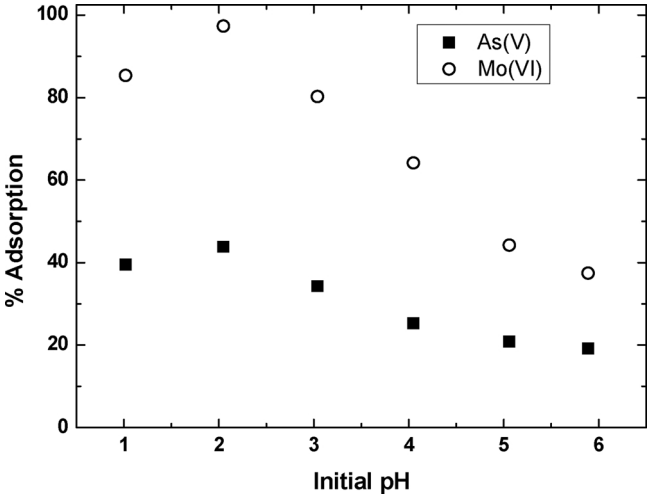

Fig. 8. Dependence of Mo(VI) and As(V) ion adsorption onto mag-MnO_2 with initial pH.

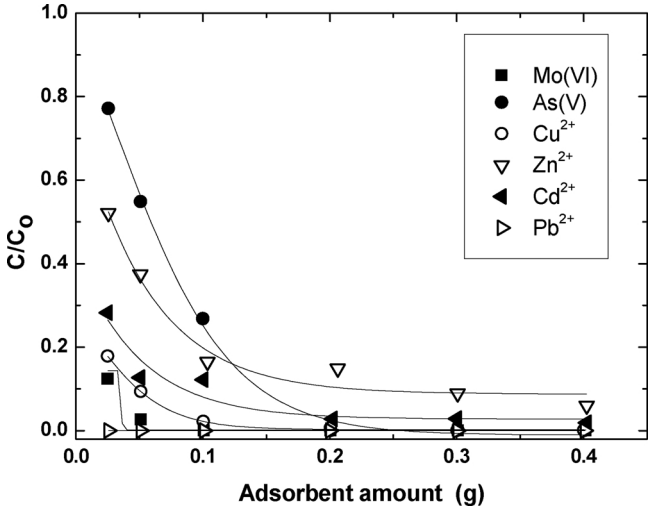

Fig. 9. Effect of adsorbent mass of mag-MnO_2 on adsorption of Pb, Cd, Cu, Zn, As, and Mo.

surface of the adsorbent would be polyprotonated, thus acquiring its positive surface charge, which would allow adsorption of anionic species by means of electrostatic attraction mechanisms and ion-pair formation, as illustrated in the following equations:

$$Mn{-}(OH)_{(s)} + H^{+}_{(aq)} \rightleftarrows Mn{-}OH^{+}_{2(s)} \quad (5)$$

$$Mn{-}OH^{+}_{2(s)} + HAO^{-}_{X(aq)} \rightleftarrows Mn{-}OH^{+}_{2} {}^{*}HAO^{-}_{X(s)} \quad (6)$$

where, HAO^{-}_{X} represents the anionic species to be removed (i.e., arsenates and molybdates). Equation 5 represents the polyprotonation of the surface of the adsorbent, and equation (6), the formation of the ion pair $-OH^{+}_{2} {}^{*}HAO^{-}_{X(s)}$.

However, according to the chemical stability tests, the pH suitable for the removal of these species should be around 2.0. Although the adsorption is still good at lower pH, the risk of its dissolution also increases. Fig. 6 shows that a better relative adsorption of molybdates with respect to arsenates under the given experimental conditions. These results could be explained by an analysis of the ionic chemical speciation of As and Mo in aqueous solutions. For example, at very low pH, As(V) can form arsenic acid (H_3AsO_4), less dissociated in arsenates, a species that would probably be adsorbed to a great extent. In turn, the predominant Mo(VI) species in aqueous solutions are the molybdate ions, which, depending on the concentration of Mo in solution and its pH, can form various anionic species. However, complete adsorption of these ions could be achieved if enough adsorbent mass was used.

In sum, besides the acidity of the aqueous phase to be treated, the relative mass of adsorbent used in the experiments strongly affected the adsorption of the ionic species present in solution. Fig. 9 shows the experimental results obtained for the adsorption of the ions from an aqueous phase with an initial pH of 3.0, containing 10 mg/L of each ion. The disappearance of ions from aqueous solution is plotted as a function of the mass of adsorbent used in the experiments, where C and C_0 represent the ion concentration at any time t and its initial concentration, respectively. These results would be related to an approximation of the saturation of the adsorption sites available on the mag-MnO_2 surface when low amounts of adsorbent are used. In this case, practically all the adsorption sites would be occupied by the metal ions, resulting in a greater mass of adsorbate removed per unit mass of adsorbent. An adequate relationship must be found between the adsorbent mass to be used and the net mass of metal to be removed, depending on the concentration of the ion and the volume of aqueous solution to be used. However, in Fig. 9, it is observed that for a certain concentration of the ions in solution (10 mg/L), the percentage of adsorption increases as the amount of adsorbent used increases. It is also evident an increasing of the adsorption of As(V) and Mo(VI) would allow a complete clean-up of the aqueous solution.

To achieve a high adsorption efficiency, a sufficient adsorbent mass is required so as to offer enough available active sites for adsorption. The ion-loading capacity q for 10 to 20 mg ion/g mag-MnO_2 was measured, and the results were comparable to or exceeded those achieved using the traditionally used adsorbents, which lacks magnetic properties. As a general conclusion, mag-MnO_2 presents excellent characteristics that allow both the removal of metal ions that form cationic species in solution, as well as anionic species, depending on the pH of the treated aqueous phase. Moreover, in all cases, the loaded adsorbent could be separated easily and completely from the aqueous raffinate using the respective magnetic saturation capacity.

Similar adsorption experiments were conducted with aqueous solutions that simulate mine water, but using the other adsorbent (i.e., the mag-NanoCSH). Previous studies reported the use of this non-magnetised compound; however, given its particle size and chemical structure, its separation from the aqueous solution after adsorption is very complex [19,23]. As reported above, the magnetic silicates synthesised in this work showed a sufficient degree of magnetic saturation, which allowed their easy and complete separation from the aqueous raffinate via a neodymium magnet. Several adsorption experiments were designed and carried out using an aqueous solution that simulated mine water containing higher concentrations than that used with the mag-MnO_2. The synthesised mag-NanoCSH/Fe_3O_4 at a 1:1 ratio was utilised as the adsorbent. Fig. 10 shows the influence of the initial pH of the aqueous solution on the adsorption of ions onto this adsorbent composite. The initial concentrations of the contaminants were 100 mg/L for Pb, Cu, and Zn; 60 mg/L for Cd; and 50 mg/L for Mo and As.

An almost quantitative adsorption of the four metallic ions was independent of the acidity of the contacted aqueous phase. This is mainly because the calcium silicates alkalize the medium very quickly, irrespective of the initial acidity of the aqueous solution, generating very stable granular precipitates in all cases. The silicates acted as a buffer, always maintaining a pH higher than 7.0 in the raffinate, preventing redissolution of the precipitates obtained. The latter pose sufficient magnetic saturation, which facilitated their separation from the resulting aqueous phase. Fig. 10 also shows that the adsorption of Mo(VI) species is reasonably high, particularly at low pH, whereas the adsorption of As(V) species is limited. The preferred adsorption of molybdenum is explicable, as the Mo(VI) species for most pH values are predominantly anionic. These species would be adsorbed onto the highly protonated surface of the adsorbent through electrostatic attraction. Furthermore, it is conceivable that the higher or lesser

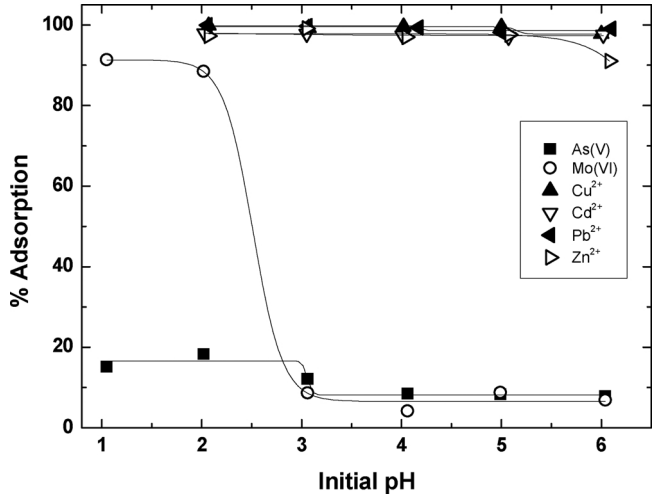

Fig. 10. Effect of pH on adsorption with mag-NanoCSH for Pb, Cd, Cu, Zn, As, and Mo.

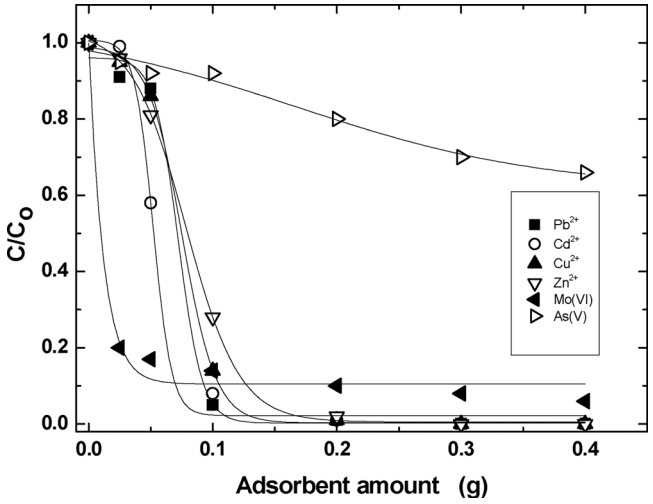

Fig. 11. Effect of adsorbent mass of mag-NanoCSH on adsorption of Pb, Cd, Cu, Zn, As, and Mo.

adsorption of anionic species by mag-NanoCSH would be related to the solubility of the respectively formed calcium salts. That is, the calcium molybdates formed would be sufficiently insoluble to allow good adsorption. The low adsorption of As(V) observed in these experiments could be explained by the low adsorbent mass used considering the vast number of species that need to be removed. Thus, higher As(V) removal can be achieved using a sufficient quantity of adsorbent. In fact, calcium arsenates and double calcium and iron arsenates are quite insoluble, which permits good adsorption, preferably at pH over 2.0, where most of the As(V) is dissociated as H_3AsO_4 [19].

A significant fraction of the heavy metals present in the AMDs is expected to precipitate when increasing the pH of the aqueous solution when lime is added. Controlled experiments were carried out using only lime to increase the pH of AMD solutions. The removal of anionic species was not good. The removal of some metallic ions, although important in many cases, in incomplete in the case of Zn, Pb, Cr among others, due to the formation of highly soluble poly-hydroxylated species and their amphoteric behaviour. Chemical precipitation with lime or limestones has many problems, such as the re-dissolution of metal precipitates, the need of huge amounts of chemicals, the generation of large volumes of colloidal sludges, etc. Precipitation with lime also provides the incomplete removal of arsenate, molybdate and sulphate ions and fails to eliminate traces of other problematic contaminants. Therefore, using only lime, it is not possible to fulfil the Chilean environmental national regulations for discharging residual mining waters to continental water bodies. In this sense, the combined use of mag-NanoCSH and mag-MnO_2 overcomes this difficulties allowing a complete and simultaneous removal of anionic and cationic species dissolved in acidic mine waters.

Several adsorption experiments were performed with variable adsorbent masses. An aqueous solution containing 100 mg/L of Pb, Cu, and Zn; 60 mg/L of Cd; and 50 mg/L of Mo and As and whose acidity was adjusted to pH 3.0 was used in all the experimental runs. The results obtained are presented in Fig. 11.

Fig. 11 shows that, in all cases, adsorption yields greater than 95% for all metal ions and Mo(VI) were achieved, with the exception of lower adsorption of arsenic species, whose complete removal was achieved with the integrated use of both magnetic adsorbents. Higher loading capacities q were measured by using mag-NanoCSH compared to mag-MnO_2 for removing the contaminant ions. In fact, q variables between 20 and 40 mg ion/g mag-NanoCSH were found, confirming that this compound should be recommended for reducing higher ion contents present in aqueous solutions in the first stage of treatment, followed by the use of mag-MnO_2 in the second stage as a polishing adsorbent for more toxic species commonly present in lower concentrations. This way, it would be possible to fulfil with the strict environmental regulations associated with acid mine waters.

When using mag-NanoCSH, metallic ions were adsorbed, most likely through combined mechanisms, such as a) by the formation of the respective hydroxide or mixed hydroxides with the silanol groups of the silicates on the surface of adsorbents and as discrete particles of hydroxides in solution, or b) via cation exchange between the adsorbed metal that becomes part of the structure of the silicate with the Ca atoms of the adsorbent, which are released to the raffinate solution. In turn, the possible mechanism of removal of anionic species as molybdates and arsenates would be governed by an anion exchange mechanism between the oxyanions existing in aqueous solution and the silicate groups of the adsorbent forming the respective calcium salt. The more insoluble the formed calcium salt with the adsorbed anion, the higher its stability, thus promoting greater adsorption and less redissolution in the resulting raffinate.

Additionally, the main reason behind conferring magnetic properties to the adsorbents is more related to achieving an easier separation of the contaminant-loaded magnetic adsorbent from the resulting aqueous solution using a conventional permanent magnet, rather than to increase their adsorption capacity. Both adsorbents do not have magnetic properties but are very good adsorbents. Furthermore, magnetite (Fe_3O_4) the compound used to provide magnetic properties to the adsorbents composites presents a very small adsorption capacity. Our control experiments indicated that magnetite only could adsorb around 2–3% of Cu and Zn, less than 1% of Cd and Pb and exhibits a null adsorption of As and Mo species. Besides, magnetite presents a PZC close to 6.0 limiting the adsorption of ionic species at pH lower than this value. It is clear that the magnetite covered with calcium silicate or hydrous MnO_2 did not affected their high adsorption capacity compared to pure calcium silicate hydrate or MnO_2 adsorbents.

Then, the magnetics composites (mag-NanoCSH and mag-MnO2) would be ideal engineered materials enabling the efficient adsorption of contaminants and the complete separation of the solids from the treated mine water.

3.4. Treatment tests of an acid mine water

The practical objective of using the adsorbents prepared in this study was the treatment of acid waters contaminated with different ionic species, both cationic and anionic. In this sense, it is required that the adsorbents ideally present capacity to remove several ions collectively and simultaneously. Using samples of a mine water generated

Table 2
Ion adsorption selectivity coefficients (α) from an acid mine water using mag-MnO_2 and mag-NanoCSH as adsorbents. Initial concentration of ions: 10 mg/L; Mass of adsorbent: 300 mg; pH 3.0.

Ions	α [mag-NanoCSH]	α [mag-MnO_2]
Pb-Cd	0.987	1.115
Pb-Cu	0.991	1.078
Pb-Zn	0.996	1.896
Cd-Cu	0.997	1.034
Cd-Zn	0.992	1.781
Cu-Zn	0.993	1.841
As-Mo	0.812	0.987
Cu-As	1.215	0.938
Zn-Mo	1.004	1.003

during Chilean copper mining activity, a series of previous experiments was conducted to measure the adsorption selectivity coefficients using both adsorbents. The selectivity coefficient represents the quotient of the respective loading capacities between a pair of ions, according to the following expression:

$$\alpha = q_a/q_b \quad (7)$$

where α is the selectivity coefficient, and q_a and q_b are the adsorption loading capacities of the metal ions *a* and *b*, respectively, both expressed in *mg adsorbed ion/g adsorbent*.

The selectivity tests were carried out using a mine water in which the concentration for each ion was adjusted in 10 mg/L and its pH to 3.0. Table 2 shows the measured values of coefficient α.

It is obvious that the closer the selectivity factor is to 1.0, the less selective the adsorbent, and therefore, the greater its capacity for collective adsorption. Although the selectivity α coefficient is sensitive to the acidity of the aqueous phase, the content of the metal ions, and the mass of adsorbent used in each case, Table 2 shows that generally both adsorbents have high collective adsorption capacity, as most of the α coefficients are close to 1.0. This is necessary for treating polluted waters containing multiple ionic contaminants. These results led us to design an integrated system using both adsorbents for cleaning up the mine waste solution.

In the first stage, the sample of the acid mine water was treated with mag-NanoCSH, which generally has a higher adsorption capacity than mag-MnO_2 does. Table 3 shows the initial concentration of all the studied ions, their concentration in the raffinate after adsorption with this compound, the extent (%) of adsorption of each species, and the limit of discharge to continental water bodies according to the Chilean National Norm [28]. Once the adsorption process, which required only a few minutes, was completed, the loaded adsorbent was completely separated from the aqueous raffinate using a neodymium magnet. Using this technique allowed us to solve one of the most complex pollution issues with the help of microadsorbents or nanoadsorbents (as their separation from the treated water is based on their magnetic properties). All the results reflect that the high adsorption achieved for all

Table 3
Treatment of an acid mine water. First step using mag-NanoCSH 1:1 as adsorbent. Initial pH: 3.0.

Element	Initial Concentration [mg/L]	Raffinate Concentration [mg/L]	Adsorption [%]	Environmental Discharge Regulation [mg/L]
Pb	10.03	0.82	91.84	0.05
Cd	11.87	0.18	98.51	0.01
Cu	52.82	0.75	98.58	1.00
Zn	43.56	0.31	99.30	3.00
As	39.07	2.87	92.66	0.60
Mo	4.75	0.33	93.05	1.00

Table 4
Treatment of the raffinate produced after adsorption of a mine water using mag-NanoCSH 1:1. Second stage using mag-MnO_2 as adsorbent.

Element	Initial Concentration [mg/L]	Raffinate Concentration [mg/L]	Environmental Discharge Regulation [mg/L]
Pb	0.82	0.033	0.05
Cd	0.18	0.008	0.01
Cu	0.75	0.127	1.00
Zn	0.31	0.01	3.00
As	2.87	< 0.45	0.60
Mo	0.33	0.14	1.00

species with this unique process can help meet the discharge regulations for copper, zinc, and molybdenum ions in acid mine waters. Furthermore, by using mag-NanoCSH, it was possible to reduce, by a very high proportion, the fine solid particles suspended in the mine water, via their adherence through coprecipitation onto the solids formed in the process.

In the second step, the aqueous raffinate produced in the first stage was mixed with the adsorbent mag-MnO_2. Although this compound had a lower adsorption capacity compared with that of mag-NanoCSH, it was useful for treating aqueous solution containing trace or lower concentrations of generally more toxic pollutants. Considering that the use of mag-NanoCSH in the first step raised the original pH of the aqueous solution to over pH 7.0, the raffinate was re-acidified with sulfuric acid to around pH 4. Table 4 shows the results of this second treatment.

The results reported in Table 4 indicate that this second adsorbent could reduce the contents of all ions in the second raffinate effectively, including the more toxic and dangerous ones, to a level below the limit fixed by the Chilean Environmental Discharge Regulation. The process was quick and, again, the loaded mag-MnO_2 compound was separated easily and completely from the resulting aqueous solution with the permanent magnet. Hence, as a global result, it is possible to state that the integrated use of both synthesised adsorbents, both prepared following a low-cost and simple process, make feasible an effective and complete decontamination treatment of acid mining water. Both adsorbents are very stable whenever the initial pH of the aqueous solutions is above 2.0 where the material losses is expected to be below 0.2-0.8 percent expressed as leaching of Fe, Ca and Mn (Fig. 6). Moreover, mechanical attrition of the adsorbents was not appreciated during the experiments. These magnetic adsorbents could also be applied for processing many kinds of residual polluted industrial waters. In a further report in preparation, we will communicate in detail the equilibrium, kinetic, and thermodynamic behaviours of both adsorbents when used in acidic solutions.

4. Conclusions

Two adsorbents with magnetic properties, based on Fe_3O_4 coated with nanostructured calcium silicate hydrate (mag-NanoCSH) and manganese oxide (mag-MnO_2), were successfully prepared with the purpose of their integrated use for remediation of an acid mine water. Both adsorbents were quite stable towards aqueous solutions with pH over 2.0, as dissolution was not observed under this condition. Both compounds were characterised using different methodologies. SEM and TEM analyses indicated that the individual particle size of the adsorbents varies between 60 and 200 nm, leading to a tendency to agglomerate. BET porosimetry analysis showed a particle surface area variable between 30 and 70 m^2/g and a pore diameter of around 2–10 nm. XRD analysis confirmed that mag-NanoCSH and mag-MnO_2 adsorbents present a crystalline magnetite nucleus surrounded by amorphous layers of calcium silicate or MnO_2, respectively. The nanostructures and microstructures of both composites showed many

available adsorption sites, and their chemical structures made them very efficient at simultaneously adsorbing both cationic and anionic species in aqueous solutions. Both adsorbents had magnetic moments of around 57–59 emu/g, which was lower than the corresponding value for Fe_3O_4 and yet high enough to ensure their complete separation from the aqueous raffinate.

The adsorption of ionic species was affected by the acidity of the aqueous solution; however, in the pH range of around 2–4, most of the contaminants were collectively removed through adsorption mechanisms based on ion exchange, ion-pair formation, and insoluble salt and hydroxide formation. The loading capacity of the adsorbents was affected by the adsorbent mass and the concentration of the species to be removed from the aqueous solution.

Both adsorbents were used in an integrated manner to decontaminate a sample of an acid mine water. mag-NanoCSH, which has a higher adsorption capacity, was used in the first step and drastically reduced the concentration of many ions present in the treated water. Consecutively, after re-acidification, the raffinate produced in the first step was mixed with mag-MnO_2, which resulted in an aqueous solution that met the Chilean environmental regulations for discharge into continental water bodies.

Acknowledgement

The authors gratefully acknowledge the financial support given by Chile/FONDECYT through research grant no. 1140331.

References

[1] M. Garcia-Lorenzo, J. Marimon, M. Navarro-Hervas, M. Navarro-Hervas, C. Perez-Sirvent, M. Martinez-Sanchez, J. Molina-Ruiz, Impact of acid mine drainages on surficial waters of an abandoned mining site, Environ. Sci. Pollut. R. 23 (2016) 6014–6023.

[2] P. Rzymski, P. Klimaszyk, W. Marszelewski, D. Borowiak, M. Mleczek, K. Nowinski, B. Pius, P. Niedzielski, B. Poniedzialek, The chemistry and toxicity of discharge waters from copper mine tailing impoundment in the valley of the Apuseni Mountains in Romania, Environ. Sci. Pollut. R. 24 (2017) 21445–21458.

[3] A. Kaksonen, C. Morris, S. Rea, J. Li, J. Wylie, F. Hilario, C. Du Plessis, Biohydrometallurgical iron oxidation and precipitation: part I - effect of pH on process performance, Hydrometallurgy 147 (2014) 255–263.

[4] D. Kolodynska, P. Rudnicki, Z. Hubicki, New approach to Cu(II), Zn(II) and Ni(II) ions removal at high NaCl concentration on the modified chelating resin, Desalin. Water Treat. 74 (2017) 184–196.

[5] A. Guimaraes, P. Da Silva, M. Mansur, Purification of nickel from multicomponent aqueous sulfuric solutions by synergistic solvent extraction using cyanex 272 and versatic 10, Hydrometallurgy 150 (2014) 173–177.

[6] O. Tavakoli, V. Goodarzi, Mohammad. Saeb, N. Mahmoodi, R. Borja, Competitive removal of heavy metal ions from squid oil under isothermal condition by CR11 chelate ion exchanger, J. Hazard. Mater. 334 (2017) 256–266.

[7] Cotorás, D., Valenzuela, F., Zarzar, M., Viedma, P., 2008. Process for the removal of metals by biosorption from mining or industrial effluents. US Pat. 7.326.344.

[8] V. Nayak, M. Jyothi, R. Balakrishna, M. Padaki, S. Deon, Novel modified poly vinyl chloride blend membranes for removal of heavy metals from mixed ion feed sample, J. Hazard. Mater. 331 (2017) 289–299.

[9] A. Lambert, P. Drogui, R. Daghrir, F. Zaviska, M. Benzaazoua, Removal of copper in leachate from mining residues using electrochemical technology, J. Environ. Manage. 133 (2014) 78–85.

[10] Y. Lee, W. Park, J. Yang, Removal of anionic metals by amino-organoclay for water treatment, J. Hazard. Mater. 190 (2011) 652–658.

[11] Y. Yang, J. Shapter, R. Popelka-Filcoff, J. Bennett, A. Ellis, Copper removal using bio-inspired polydopamine coated natural zeolites, J. Hazard. Mater. 273 (2014) 174–182.

[12] N. Negm, R. El Sheikh, A. El-Farargy, H. Hefni, M. Bekhit, Treatment of industrial wastewater containing copper and cobalt ions using modified chitosan, J. Ind. Eng. Chem. 21 (2015) 526–534.

[13] M. Anbia, Z. Ghassemian, Removal of Cd(II) and Cu(II) from aqueous solutions using mesoporous silicate containing zirconium and iron, Chem. Eng. Res. Des. 89 (2011) 2770–2775.

[14] L. Westholm, E. Repo, M. Sillanpaa, Filter materials for metal removal from mine drainage-a review, Environ. Sci. Pollut. R. 21 (2014) 9109–9128.

[15] W. Olds, D. Tsang, P. Weber, Acid mine drainage treatment assisted by lignite-derived humic substances, Water Air Soil Pollut. 224 (2013) 1521–1525.

[16] B. Pan, Z. Li, Y. Zhang, J. Xu, L. Chen, H. Dong, W. Zhang, Acid and organic resistant nano-hydrated zirconium oxide (HZO)/polystyrene hybrid adsorbent for arsenic removal from water, Chem. Eng. J. 248 (2014) 290–296.

[17] A. Rahmani, H. Mousavi, M. Fazli, Effect of nanostructure alumina on adsorption of heavy metals, Desalination 253 (2010) 94–100.

[18] S. Salem, A. Salem, A novel design for clean and economical manufacturing new nano-porous zeolite based adsorbent by alkali cement kiln dust for lead uptake from wastewater, J. Clean. Prod. 143 (2017) 440–451.

[19] K. Barrera, A. Briso, V. Ide, L. Martorana, G. Montes, C. Basualto, T. Borrmann, F. Valenzuela, Treatment of mine acid waters by an adsorption process using calcium silicate modified with Fe(III), Hydrometallurgy 172 (2017) 19–29.

[20] S. Tang, P. Wang, K. Yin, I. Lo, Synthesis and application of magnetic hydrogel for Cr(VI) removal from contaminated water, Environ. Eng. Sci. 27 (2010) 947–954.

[21] D. Mehta, S. Mazumdar, S. Singh, Magnetic adsorbents for the treatment of water/wastewater. A review, J. Water Proc. Eng. 7 (2015) 244–265.

[22] C. Basualto, P. González, A. Briso, K. Barrera, V. Ide, M. Araya, G. Montes, F. Valenzuela, Synthesis and use of nano magnetic MnO2 adsorbent for removing Pb (II) and Cd(II) ions from acid aqueous solutions, Desalin. Water Treat. 70 (2017) 175–182.

[23] F. Valenzuela, C. Basualto, J. Sapag, V. Ide, N. Luis, N. Narvaéz, S. Yañez, T. Borrmann, Adsorption pf pollutant ions from residual aqueous solutions onto nano-structured calcium silicate, J. Chil. Chem. Soc. 58 (2013) 1553–1558.

[24] C. Calderón, M. Franzreb, F. Valenzuela, W. Höll, Magnetic manganese dioxide as an amphoteric adsorbent for removal of harmful inorganic contaminants from water, React. Funct. Polym. 70 (2010) 516–520.

[25] C. Basualto, J. Gaete, L. Molina, F. Valenzuela, C. Yañez, J. Marco, Lanthanide sorbent based on magnetite nanoparticle functionalized with organophosphorus extractants, Sci. Technol. Adv. Mater. 16 (2015) 035010, , https://doi.org/10.1088/1468-6996/16/3/035010 (9pp).

[26] M. Cairns, T. Borrmann, W. Höll, J. Johnston, A study of the uptake of copper ions by nanostructured calcium silicate, Microporous Mesoporous Mater. 95 (2006) 126–134.

[27] S. Thurm, S. Odenbach, Particle size distribution as key parameter for the flow behavior of ferrofluids, Phys. Fluids 15 (2003) 1658–1664.

[28] Norm, N° 90/2000 Maximum allowable limits for discharge of liquid wastes to continental and marine surface waters, Minister of General-Secretary of Presidence, Chile Government, 2001.